Lattice dynamics of mercury(II)iodide

Lydia Nemec
University of Regensburg

Supervisor:
Dieter Strauch

ESDG, 19th May 2010

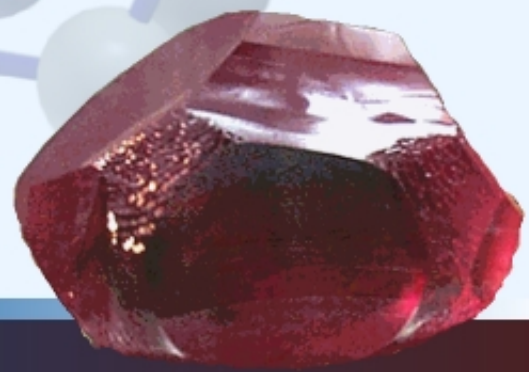

Lattice dynamics of mercury(II)iodide

- Motivation
- Method
- Geometry
- Electronic Structure
- Lattice Dynamics
- Scattering Spectra
- Conclusions and Outlook

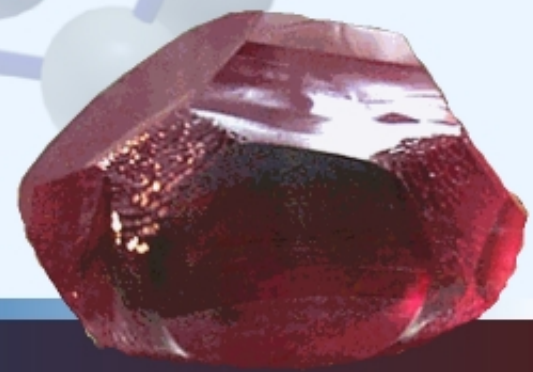

Motivation

- Mercury(II)iodide (HgI_2) is an important material for X- and γ-ray detection at room temperature.
  - High quality crystals are difficult to grow.
  - Vibrational properties have been studied experimentally and theoretically in two of three symmetry directions.
  - Full experimental phonon data are not available.

- Computer simulation to support neutron scattering experiment

Lattice dynamics of mercury(II)iodide

- Motivation
- Method
- Geometry
- Electronic Structure
- Lattice Dynamics
- Scattering Spectra
- Conclusions and Outlook

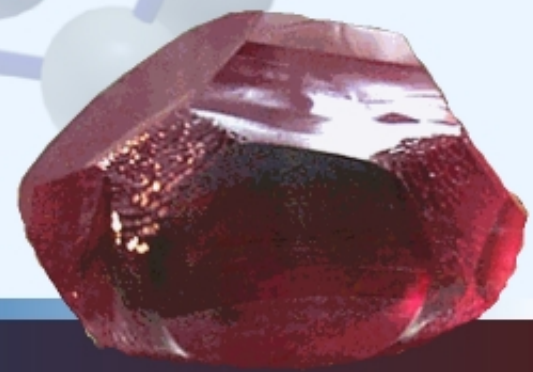

Method: Density Functional Theory

ABINIT[1], SIESTA[2] and Pseudopotentials

- Total energy E_{tot} and density $n(\vec{r})$ as a function of Kohn-Sham wavefunctions $\varphi_i(\vec{r})$

$$E_{tot} = \sum_{\alpha}^{occ} \langle \varphi_i | T + v_{ext} | \varphi_i \rangle + E_{H_{xc}}[n(\vec{r})] \qquad n(\vec{r}) = \sum_{\alpha}^{occ} \varphi_i^{cc}(\vec{r}) \varphi_i(\vec{r})$$

- solve Kohn-Sham equations self-consistently

Code	ABINIT	SIESTA
Basis	Plane Wave basis Cut-off Energy: 700 eV	Numerical atomic orbitals basis set Optimized with SIMPLEX[4]
XC - functional	GGA	GGA
Pseudopotential	Optimized Pseudopotential Generated by OPIUM[3]	Kerker Pseudopotential Generated bei ATOM[2]
Used for	Electronic structure and phonons	Electronic structure

1 X. Gonze et al.; Z. Kristallogr. 220, 558–562 (2005)
2 J. Soler, M. E. Artacho, J. D. Gale, A. García, J. Junquera, P. Ordejòn, D.J. Sànchez-Portal; Phys: Condens Matter 14, 2745 (2002)
3 A. M. Rappe, K. M. Rabe, E. Kaxiras, J. D. Joannopoulos; Phys. Rev. B 41, 1227 (1990)
4 E. Anglada, J. M. Soler, J. Junquera, M. E. Artacho; Phys Rev B 66, 205101 (2002)

Method: Phonons

- **So far:** total energy with fixed position of the atoms → Born-Oppenheimer Approximation
- **Now:** add atomic vibrations → expansion of the total energy around the equilibrium geometry

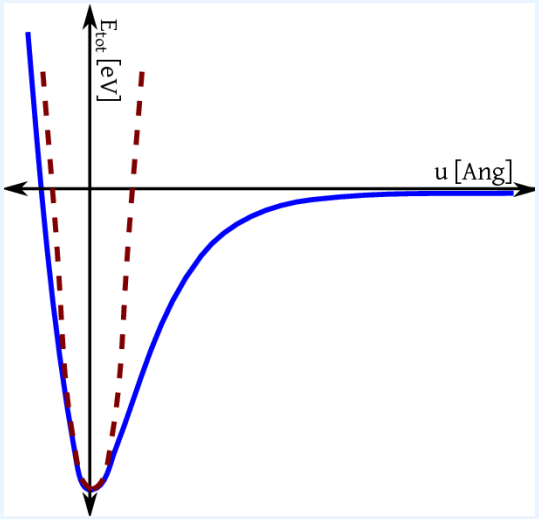

cell a — Equilibrium position of Atom α — displacement of Atom α in direction i

$$R^a_{i\alpha} = R^a_i + \tau_{i\alpha} + u^a_{i\alpha}$$

$$E^{harm}_{tot}(\boldsymbol{u}) = E^{(0)}_{tot} + \frac{1}{2}\sum_{i\alpha a}\sum_{j\alpha' a'} \underbrace{\left(\frac{d^2E}{du^a_{i\alpha}\, du^{a'}_{j\alpha'}}\right)}_{=: C_{i\alpha,j\alpha'}(a,a')} u^a_{i\alpha}\, u^{a'}_{j\alpha'}$$

force constant matrix (FCM)

- The **Fourier transformed FCM:** $\overline{C}_{i\alpha,j\alpha'}(\vec{q}) = \sum_{i\alpha,j\alpha'} C_{i\alpha,j\alpha'}(0,a')\, e^{i\vec{q}\vec{R}_{a'}}$
  - The **full solution of vibrational states:** $det\left|\bar{D}(\vec{q}) - \omega^2\right| = 0$
  - The **dynamical matrix** $\overline{D}_{i\alpha,j\alpha'}(\vec{q}) = \frac{\overline{C}_{i\alpha,j\alpha'}(\vec{q})}{\sqrt{M_i' M_j}}$

Method:

Phonons – Task find the dynamical Matrix

- **Frozen Phonons:** Frequencies of selected phonon modes are calculated from differences in the total energy and forces acting on a nuclei "frozen" at position R_i produced by finite, periodic displacements of a few atoms in an otherwise perfect structure at equilibrium. A frozen phonon calculation for lattice vibrations at a generic reciprocal-lattice vector $\vec{q}$ requires a supercell. The size of the supercell must be at least equals phonon wavelength.

  Long-range polarization fields are not compatible with the periodic boundary conditions for supercells. Hence, the long-range polarization fields are artificially suppressed in supercells resulting in a vanishing LO-TO splitting. Long-range fields can be handled via the asymptotic behaviour of planar force constants between very distant planes, requiring very extended supercells.

- **Density Functional Perturbation Theory:** DFPT avoids the problem of large supercells. Within this approach one starts from the ground state results obtained for the primitive unit cell. The response to arbitrary infinitesimal displacements of the atoms and to corresponding changes of the ionic potential is calculated by means of perturbation theory. The derivatives are taken at equilibrium positions, i.e., use of full symmetry.

  Another advantage is the rigorous inclusion of long-range polarization fields introduced by LO phonons near the Gamma-point in ionic semiconductors resulting in a LO-TO splitting near Gamma.

Method: Density Functional Perturbation Theory DFTP

$$E_{tot} = \sum_{\alpha}^{occ} \langle \varphi_i | T + v_{ext} | \varphi_i \rangle + E_{H_{xc}}[n(\vec{r})]$$

Perturbation in the crystal structure → change in the external potential
Expand perturbed potential in a small parameter λ:

$$v_{ext}^{\lambda} = v_{ext}^{(0)} + \lambda\, v_{ext}^{(1)} + \frac{1}{2}\lambda^2 v_{ext}^{(2)} + O(\lambda^3)$$

The perturbed quantities E_{tot}^{λ}, $\varphi_i^{\lambda}(\vec{r})$, $n(\vec{r})$ are expanded in the same way

Hellmann-Feynman theorem → $\frac{\partial E_{tot}}{\partial \lambda}$ depends only on $n^{(0)}(\vec{r})$

$$\frac{\partial^2 E}{\partial \lambda^2} = \int d^3 r \frac{\partial v_{ext}^{\lambda}(\vec{r})}{\partial \lambda} \cdot n^{(1)}(\vec{r}) + \int d^3 r\, n^{(0)}(\vec{r}) \frac{\partial^2 v_{ext}^{\lambda}(\vec{r})}{\partial \lambda^2}$$

$(2n+1)$-theorem[1] → set of equations to be solved self-consistently

1 X. Gonze and J. Vigneron, Physical Review B 39, 13120 (1989)

Method: Density Functional Perturbation Theory DFTP

Solve self-consistently for any fixed vector $\vec{q}$: start with initial guess for $H^{(1)}$

- From $H^{(1)}$ calculate $\varphi^{(1)}_i$ by solving

$$\left(H^{(0)}-\epsilon_i\right)|\varphi_i^{(1)}>.=-P_c H^{(1)}|\varphi_i^{(0)}>.$$

$$P_c=1-\sum_{i=1}^{N}|\varphi_i><\varphi_i|$$

- The first order density is given by

$$n^{(1)}(\vec{k})=\varphi_i^{cc(1)(\vec{k}+\vec{q})}\varphi_i^{(0)\vec{k}}+\varphi_i^{cc\,(0)\vec{k}}\varphi_i^{(1)(\vec{k}+\vec{q})}$$

- Build new perturbed Hamiltonian

$$H^{(1)}=v_{ext}^{(1)}+v_{H_{xc}}=v_{ext}^{(1)}\mathrm{e}^{i\vec{q}\cdot\vec{r}}+\int dr'\left.\frac{\partial^2 E_{H_{xc}}}{\partial n(\vec{r})\partial n(\vec{r})}\right|_{n^{(0)}}\cdot n^{(1)}(\vec{r}\,')+\frac{d}{d\lambda}\frac{\partial E_{H_{XC}}}{\partial n(\vec{r}\,')}$$

- Repeat until a desired accuracy is reached

Lattice dynamics of mercury(II)iodide

- Motivation
- Method
- Geometry
- Electronic Structure
- Lattice Dynamics
- Scattering Spectra
- Conclusions and Outlook

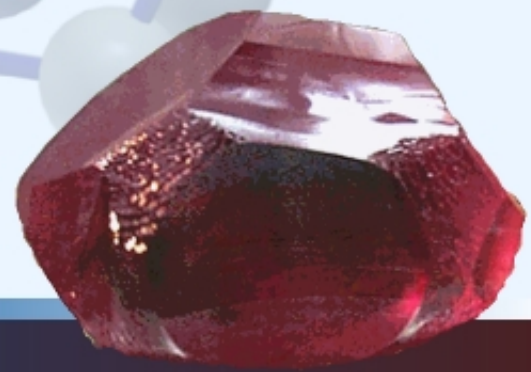

Geometry

The Geometry of HgI_2

- Tetragonal system
- Space group: $P4_2/nmc$
- Distorted by ***u*** from an ideal cubic close packing

Code	x = y [Å]	z [Å]	u	D(I – I)[Å]
ABINIT	4.426	13.259	0.130	0.240z
SIESTA	4.214	12.124	0.134	0.231z
WIEN97[1]	4.577	13.583	0.128	0.244z
Experiment				
Jeffrey et al.[2]	4.361	12.450	0.139	0.22z
Nicolau et al.[3]	4.374	12.435	0.139	0.222z

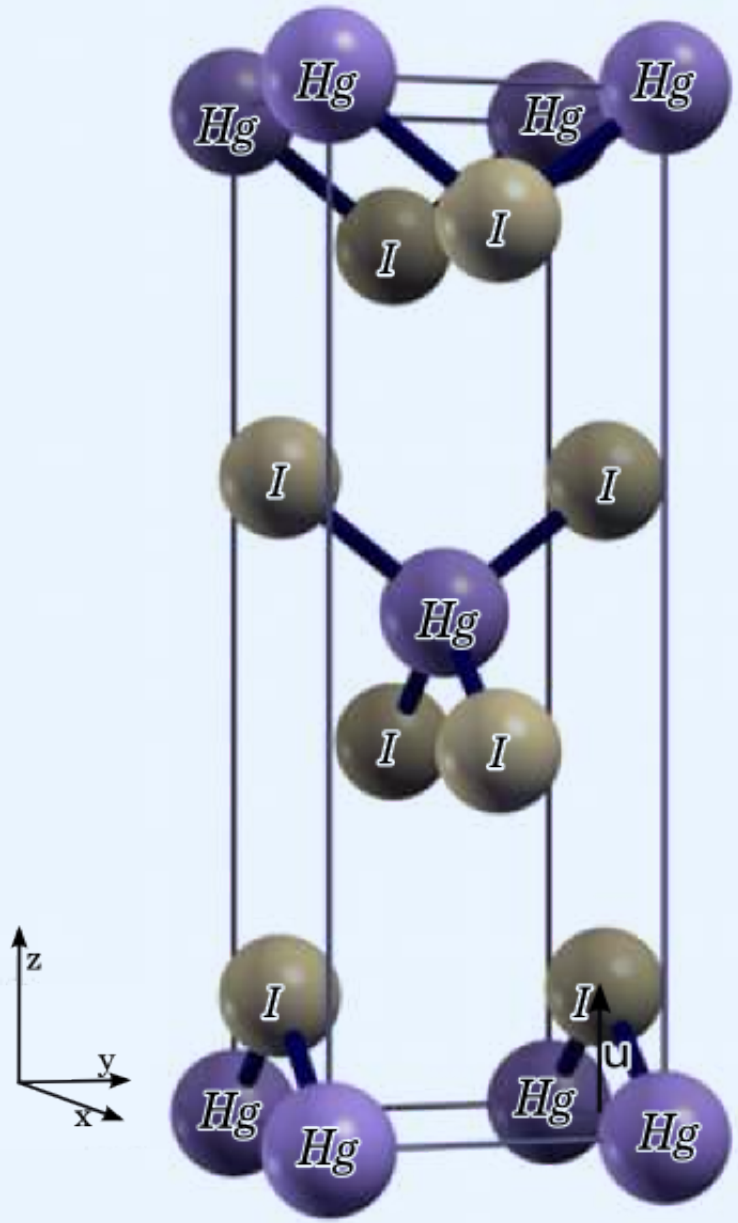

1 F. Ayres, L. V. C. Assali, W. V. M. Machado and J. F. Justo, Brazilian Journal of Physics 34, 681 (June 2004)
2 G. A. Jeffrey and M. Vlasse, Inorganic Cemistry 6, 396 (Feb. 1967)
3 Y. F. Nicolau, M. Dupuy and Z. Kabsch, Nuclear Instruments and Methods in Physics Research Section A 283, 149 (1989)

Lattice dynamics of mercury(II)iodide

- Motivation
- Method
- Geometry
- Electronic Structure
- Lattice Dynamics
- Scattering Spectra
- Conclusions and Outlook

Electronic Structure:

Comparison between SIESTA, ABINIT previous results

- The band gap depends sensitively on the total pressure of the unit cell
- Only the calculations from Ayres et al. took into account geometry optimization
- The band gap was underestimated using 37.6% by ABINIT

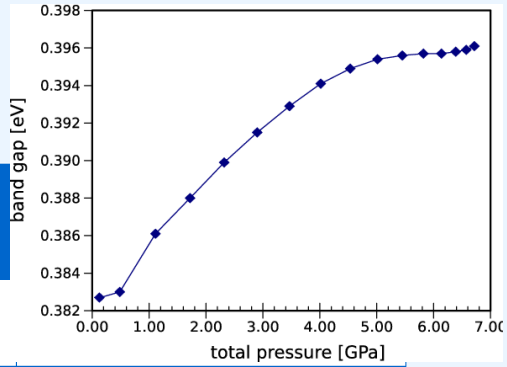

Code	Siesta relaxed Unit Cell	Siesta fixed Unit Cell	ABINIT relaxed Unit Cell
Band gap [eV]	0.38	0.396	1.33

Experiment/ Theory	Piechotka[1]	Turner et al.[2]	Solanki et al.[3]	Ayres et al.[4]
	Experiment	Muffin-tin orbital calculation (LDA)	Scalar relativistic linear muffin-tin orbital	All-electron, full-potential LAPW incl. Spin-Orbit
Band gap [eV]	2.13	0.52	0.95	0.98

1 M. Piechotka; Materials Science and Engineering: R: Reports 18, 1-98 (1997)
2 D. E. Turner and B. N. Harmon; Phys. Rev. B 40 (15), 10516 (1989)
3 A. K. Solanki, A. Kashyap, T. Nautiyal, S. Auluck, M. A. Khan; Phys. Rev. B 55 (15), 9215 (1997)
4 F. Ayres, L. V. C. Assali, W. V. M. Machado and J. F. Justo; Brazilian Journal of Physics 34, 681 (June 2004)

Electronic Structure:

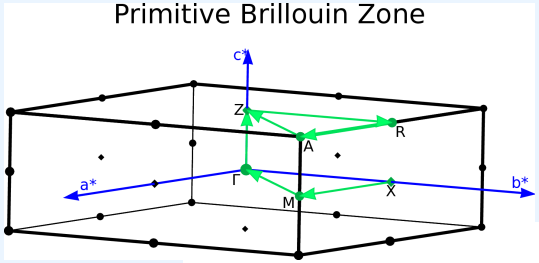

Band Structure for HgI_2

Density of States HgI_2

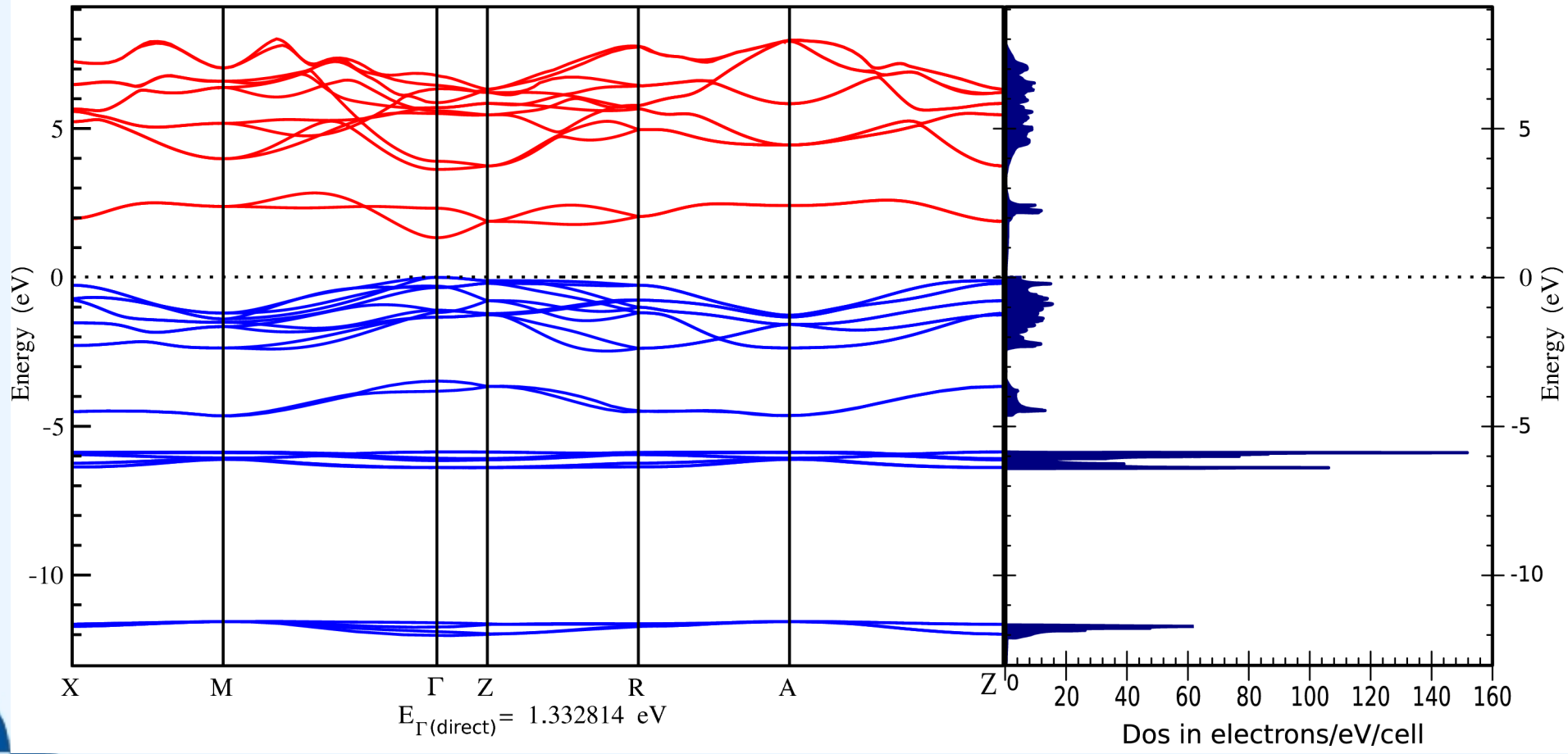

Lattice dynamics of mercury(II)iodide

- Motivation
- Method
- Geometry
- Electronic Structure
- Lattice Dynamics
- Scattering Spectra
- Conclusions and Outlook

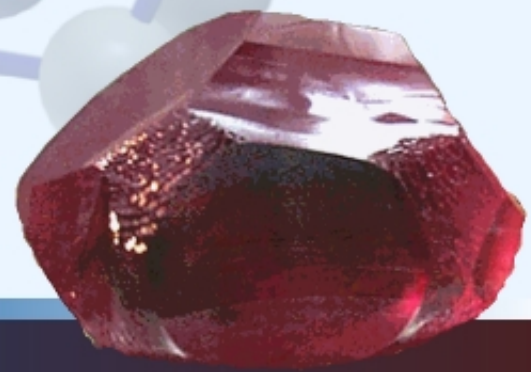

Lattice dynamics: The dielectric constant

- HgI_2 is an ionic crystal
- $Hg^{+2\delta}$ and $I^{-\delta}$ ions are moved against each other → Results in a macroscopic polarisation $\vec{P}$

$$\vec{P} = \frac{1}{v} \sum_i^N Z_i^* \vec{u}_i$$

$v \ldots unit\ cell\ volume$
$N \ldots number\ of\ atoms$
$Z_i^* \ldots Born\ effective\ charge\ of\ atom\ i$

$$\vec{E}_{mac} = -4\pi \frac{(\vec{k} \cdot \vec{P})}{\vec{k}^2} \vec{k}$$

- $\vec{E}_{mac}$ is a macroscopic electric field where $\vec{k}$ is the wave vector
- Calculated Born effective charges for α-HgI_2

		Hg	I_x	I_y	I_z
Experiment Bielmann and Prevot[1]	$Z^*_{.\parallel\vec{E}}$	2.227	---	---	---
	$Z^*_{.\perp\vec{E}}$	3.06	---	---	-1.53
ABINIT Relaxed UC	$Z^*_{.\parallel\vec{E}}$	2.765	-0.455	-2.310	---
	$Z^*_{.\perp\vec{E}}$	1.706	---	---	-0.853
ABINIT Exp UC	$Z^*_{.\parallel\vec{E}}$	2.752	-0.434	-2.318	---
	$Z^*_{.\perp\vec{E}}$	2.074	---	---	-1.037
SIESTA relaxed UC	$Z^*_{.\parallel\vec{E}}$	2.771	-0.429	-2.342	---
	$Z^*_{.\perp\vec{E}}$	2.488	---	---	-1.244

Lattice dynamics:

The dielectric constant

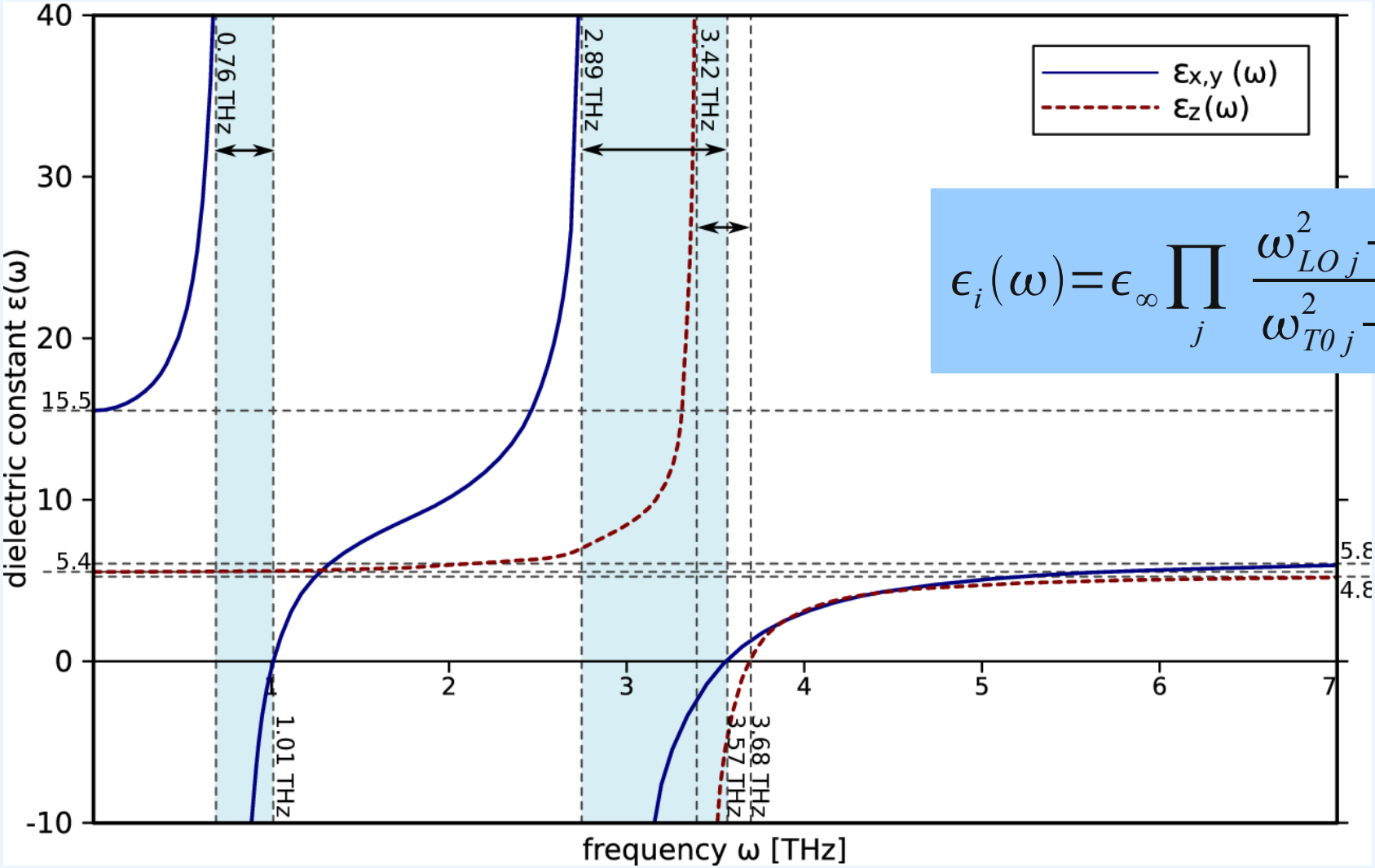

$$\epsilon_i(\omega) = \epsilon_\infty \prod_j \frac{\omega_{LO\,j}^2 - \omega^2}{\omega_{T0\,j}^2 - \omega^2}$$

The frequency dependent dielectric constant ε(ω)

Lattice dynamics:

Phonon modes at the Gamma point

- The irreducible representations: $(A_{1g}, 2A_{2u}, B_{2u}, B_{1g}, 3E_g, 3E_u)$
- Inversion symmetry → even mode (g) differs from corresponding odd mode (u) by an interlayer phase shift of 180°
- Davidov pairs: pair of even and odd mode
- Raman and Infrared active modes are mutually exclusive

Lattice dynamics:

Phonon modes at the Gamma point

acoustical	acoustical	infrared	inactive	infrared	infrared
non-degenerate	doubly degenerate	doubly LO-TO	non-degenerate	doubly LO-TO	non-degenerate
0.000 THz	0.000 THz	TO 0.762 THz LO 1.010 THz	2.940 THz	TO 2.892 LO 3.566	TO 3.422 THz LO 3.682 THz

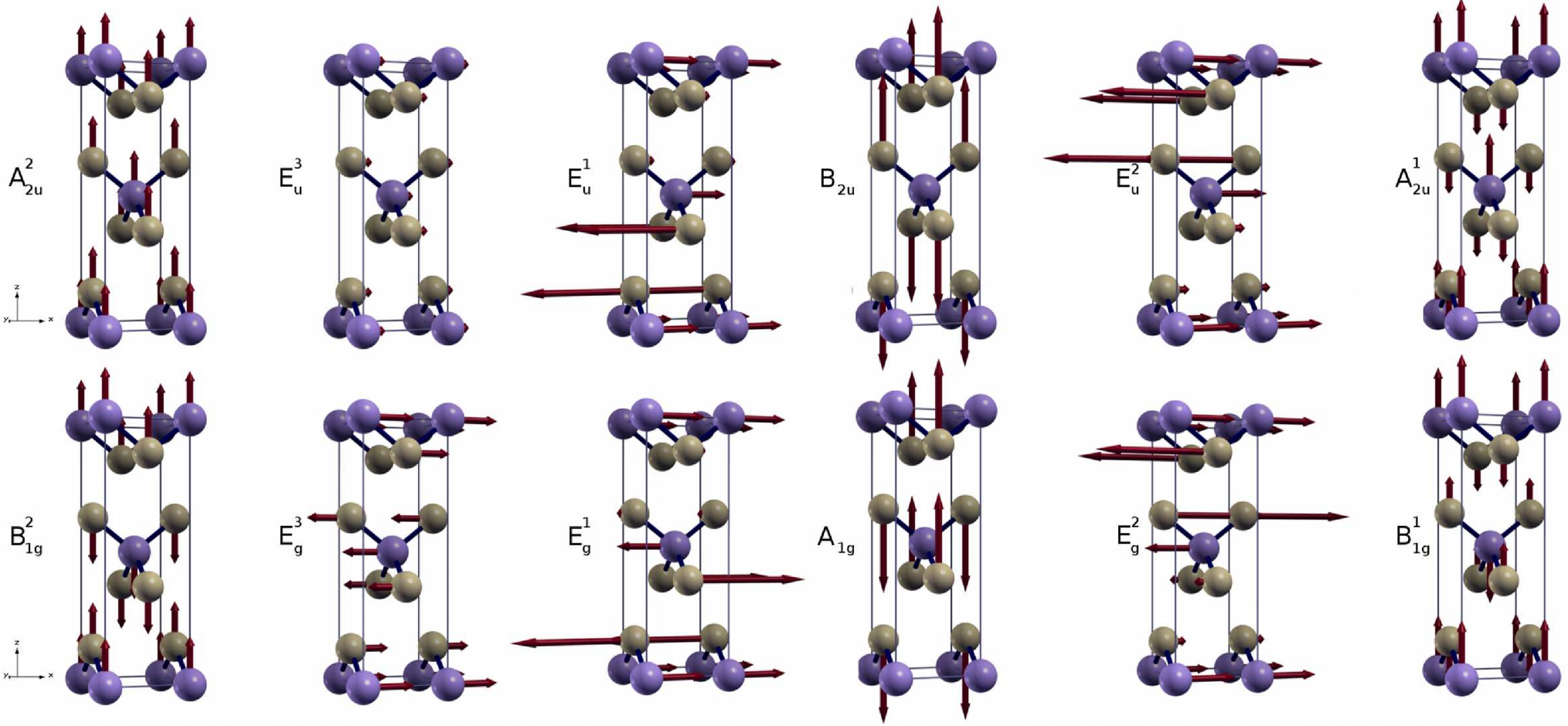

Raman	Raman	Raman	Raman	Raman	Raman
non-degenerate	doubly degenerate	doubly degenerate	non-degenerate	doubly degenerate	non-degenerate
0.359 THz	0.270 THz	0.812 THz	2.952 THz	2.983 THz	3.690 THz

Lattice dynamics: Angle dependence in Gamma and LO-TO Splitting

- Transversal modes E^2_u and E^1_u split into transverse optical and longitudinal optical mode
- E^1_u changes polarisation, but not the symmetric presentation
- Longitudinal A^1_{2u} mode changes its frequency due to the electric field
- Electric field perpendicular energy is maximised

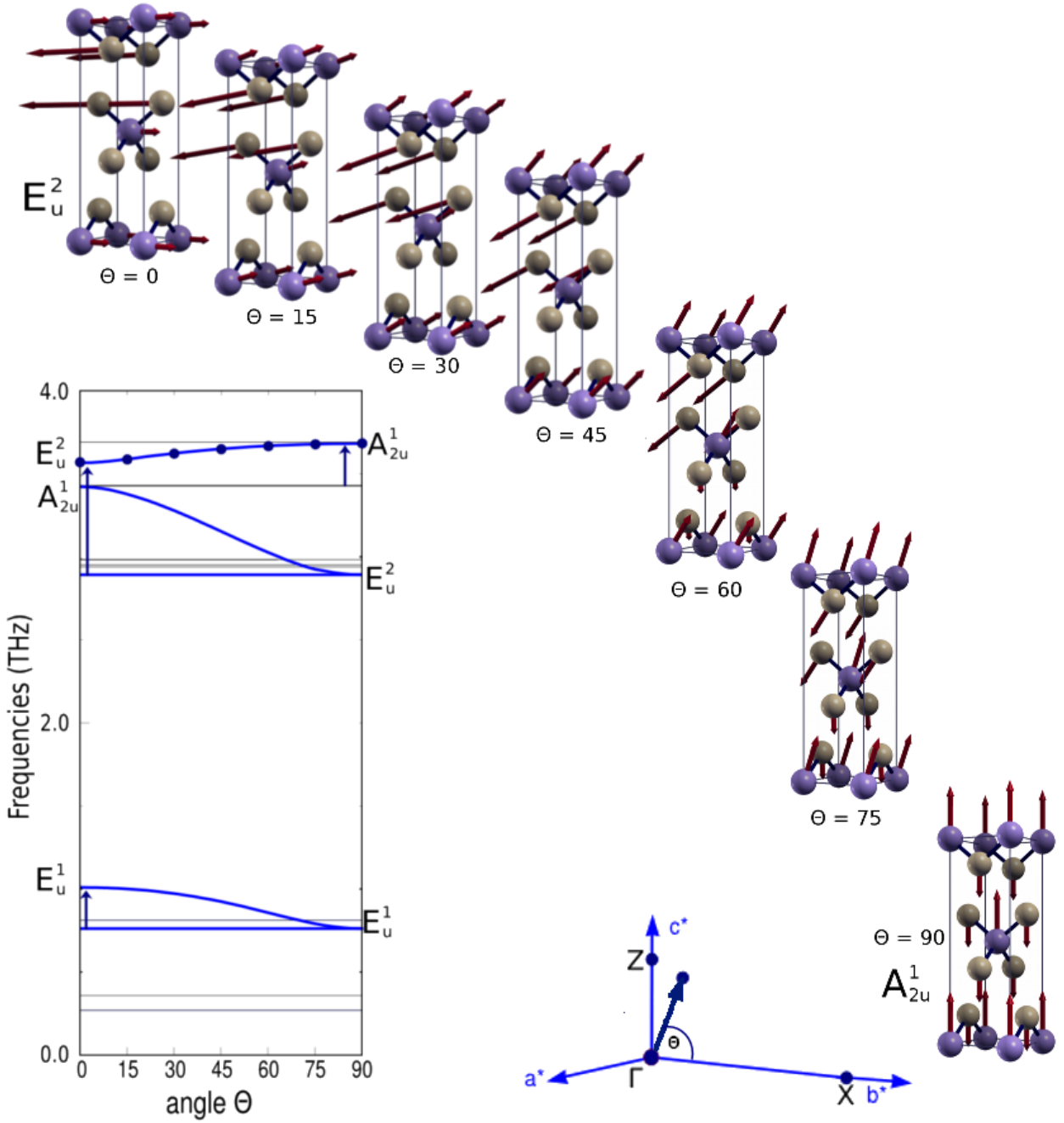

Lattice dynamics:

Phonon dispersion in the [100], [001] and [110]- plane

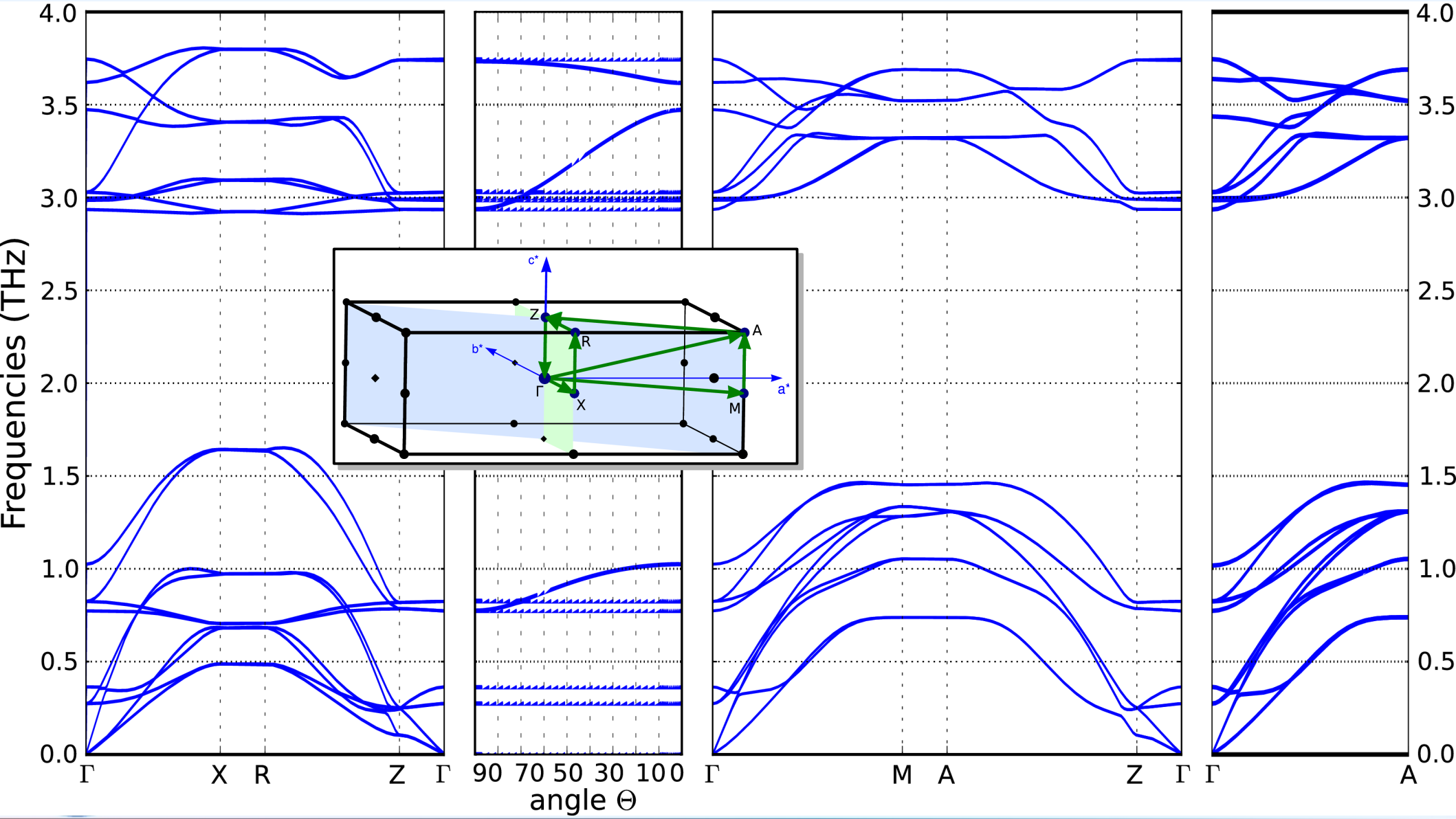

Lattice dynamics of mercury(II)iodide

- Motivation
- Method
- Geometry
- Electronic Structure
- Lattice Dynamics
- Scattering Spectra
- Conclusions and Outlook

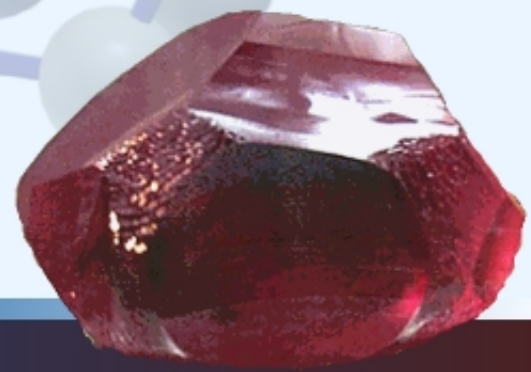

Streuintensitäten:

Comparison between experiment and theory

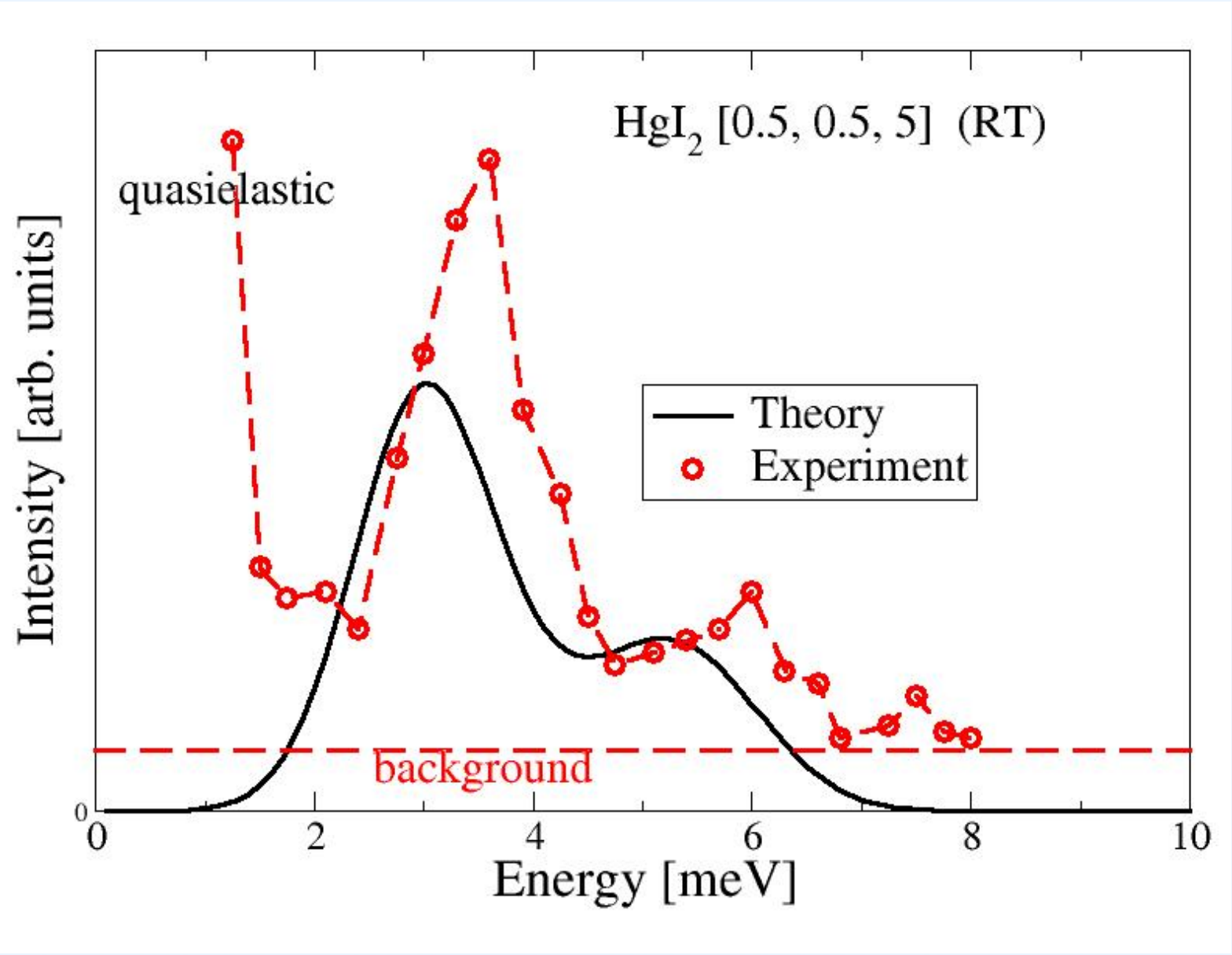

Lattice dynamics of mercury(II)iodide

- Motivation
- Method
- Geometry
- Electronic Structure
- Lattice Dynamics
- Scattering Spectra
- Conclusions and Outlook

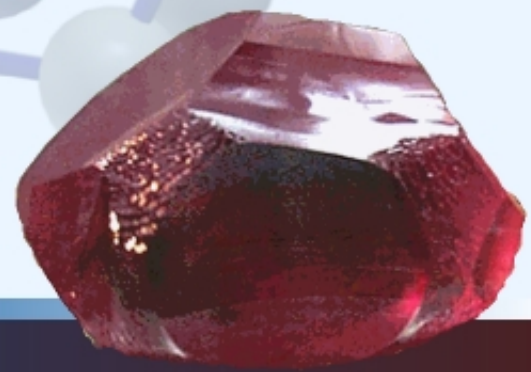

Conclusions:

- Geometry and band gap: excellent agreement with experiment (better than previously published results)
- Detailed discussion of the LO-TO splitting of the optical modes
- First ab initio results for phonon dispersion in the [100] and [001]-plane: comparable with published data
- Phonon dispersion of the so far unpublished [110]-plane

Outlook

- Neutron scattering experiment planned